Performance evaluation of a counter-rotating tidal turbine using Blade Element Theory

Song Fu and Cameron Johnstone

Abstract— **This research paper presents an investigation into the performance evaluation of a counter-rotating tidal turbine. The evaluation is based on the utilization of the Blade Element Momentum Theory (BEMT) as the analytical framework. A crucial aspect in solving the model lies in accurately defining the inflow velocities for both the front and rear rotors. Specifically, the inflow velocity experienced by the rear rotor is contingent upon the wake generated by the front rotor. To address this, a Gaussian-shaped velocity deficit wake model has been applied in conjunction with the BEMT methodology. Subsequently, once the inflow velocities for both the front and rear turbines have been ascertained, the dynamics of the counter-rotating turbine can be effectively simulated within the BEMT model.**

Keywords— Counter-rotating, BEMT, tidal turbine.

I. INTRODUCTION

THIS paper aims to summarize a method to simulate the counter-rotating tidal turbines (CRTTs) with Blade Element Momentum Theory (BEMT) and predict their hydrodynamic performance. CRTTs are a type of tidal turbine with two rotors rotating in opposite directions, which presents a more complex phenomenon arising from the hydrodynamic interaction between the two rotors. This review highlights several studies that investigate the aerodynamic performance of counter rotating wind turbines (CRWTs) and hydrodynamic performance of CRTTs using various methods such as free-wake vortex lattice method, quasi-steady strip theory, and computational fluid dynamics (CFD) simulation.

Lee et al. [1] conducted an aerodynamic analysis of a CRWT using a free-wake vortex lattice method to consider the aerodynamic interaction between the two rotors. Hwang et al. [2] optimized the pitch angles, radius ratios, and rotation speeds of two rotors to observe the variations of the power coefficients and thrust coefficients. Wei et al. [3] conducted a series of experiments in a wind tunnel to investigate the influence of blade pitch angle and axial distance on the performance of the CRWT. Huang et al. [4] developed a CFD model using block-structured grid and performed an experimental test in a water tunnel for a tidal stream turbine with counter-rotating type propellers. Huang [5] also studied numerical and experimental analysis of a CRTT.

Dong et al. [6] predicted the aerodynamic performance of a 30kW CRWT system using the momentum theory and two-dimensional quasi-steady strip theory. Jung et al. [7] investigated the aerodynamic performance prediction of a unique 30kW CRWT system, consisting of the main rotor and the auxiliary rotor, using the quasi-steady strip theory. Lee et al. [8] developed a modified blade element momentum theory for the CRWT to investigate the effects of various design parameters on its aerodynamic performance. Abohamzeh et al. [9] investigated the aerodynamic and aeroacoustic performance of a CRWT using CFD simulation.

Furthermore, this review highlights studies conducted on wind-turbine wakes that influence the performance of CRWTs. Bastankhah et al. [10] proposed a new analytical wake model to predict the wind velocity distribution downwind of a wind turbine. Abkar et al. [11] investigated the influence of atmospheric thermal stability on wind-turbine wakes using large-eddy simulation combined with a turbine model. Ge et al. [12] proposed a two-dimensional (2D) wake model that conserves mass locally and globally.

Song Fu is at Energy Systems Research Unit, Department of Mechanical and Aerospace Engineering, University of Strathclyde, Glasgow, UK, G1 1XJ (e-mail: song.fu@strath.ac.uk).

Cameron Johnstone is at Energy Systems Research Unit, Department of Mechanical and Aerospace Engineering, University of Strathclyde, Glasgow, UK, G1 1XJ (e-mail: cameron.johnstone@strath.ac.uk).

Digital Object Identifier: https://doi.org/10.36688/ewtec-2023-506

II. NUMERICAL METHOD

The blade element momentum theory (BEMT) is a widely recognized methodology that combines the momentum theory and blade element theory for the purpose of rotor analysis. The momentum theory, based on the conservation of linear and angular momentum within a control volume, is coupled with the blade element theory, which is grounded in the lift and drag characteristics of the airfoil shape of blade sections, to

provide a comprehensive and robust framework for rotor analysis. Specifically, the blade element theory assumes that there is no aerodynamic interaction between section elements. By applying BEMT, it is possible to determine the inflow on each blade section by equating the forces generated by the two aforementioned theories. Due to its solid physical underpinnings and relatively low computational cost, BEMT has emerged as a reliable and effective theory for rotor design.

The counter-rotating tidal turbine has two rotors rotating in opposite directions on the same axis. It has been proposed on the basis of the theory which states that a configuration of two rotors having the similar swept area on the same axis has a higher maximum power coefficient than a conventional configuration of a wind turbine with a single rotor.

The flow model for the counter-rotating wind turbine is shown in Fig. 1. The rear turbine operates in the wake of the front turbine at plane 3 (U_{W3}). Moreover, the inflow velocity of the rear turbine is also affected by the rear turbine according to Wei's study [13], this term is defined as self-induced velocity of the rear turbine at plane 2 (U_{2i}) in this paper.

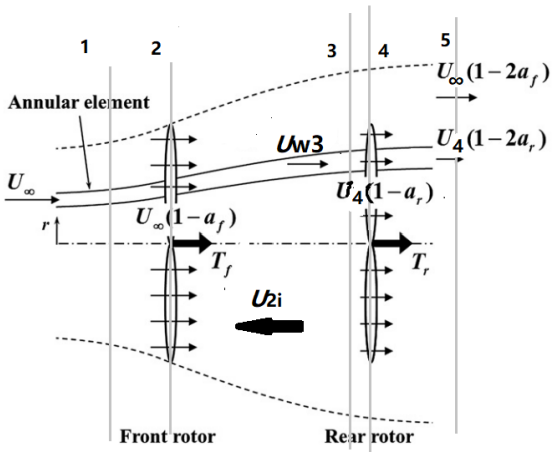

Fig. 1. Flow model of the BEMT for a counter-rotating wind turbine with the rear rotor operating inside the stream tube of the front rotor.

Ge et al. [12] presents a two-dimensional (2D) wake model that effectively and consistently preserves mass at both local and global scales. A direct extension of the Jensen model [14], this novel approach incorporates the wake decay rate as the sole model parameter. Furthermore, this model accounts for the pressure recovery region, which is often neglected in conventional wake models. As a result, the proposed model is capable of delivering precise predictions of the velocity deficit behind a wind turbine. Ge and his colleagues modified Bastankhah's model [10] which shown in Fig. 2 to obtained a revised model called Revised Mass Conservation Gaussian shape (RMCG) as:

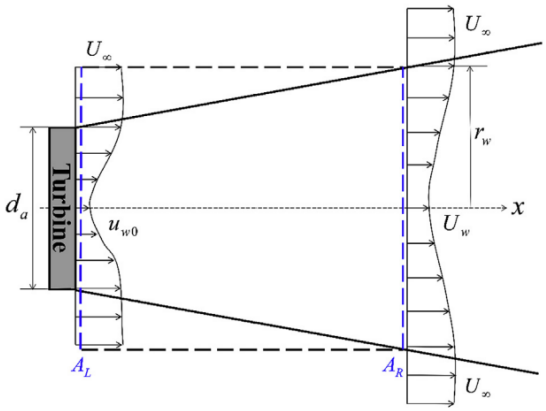

Fig. 2. Schematic of the control volume for the present 2D model with a Gaussian shaped wake deficit [12].

$$\frac{U_{W3}}{U_\infty} = 1 - \frac{2\beta\left(1-\sqrt{1-C_T/\beta}\right)}{(r_w/r_a)^2} \cdot exp\left[-\frac{2}{(r_w/r_a)^2}\left(\frac{r}{r_a}\right)^2\right] \quad (1)$$

$$\beta \equiv \frac{1+\sqrt{1-C_T}}{2\sqrt{1-C_T}} \quad (2)$$

where $r_a = d_a/2$, $r_w = kx + r_a$, x is the distance between two rotors, k is wake decay coefficient and set to be 0.075 according to [12] and C_T is the thrust coefficient.

For the counter rotating turbine, the variable x is equal to the distance between two rotors.

The original thrust and torque of the front turbine are

$$\mathrm{d}T_f = 4\rho U_\infty^2 a_f(1-a_f)\pi r \mathrm{d}r \quad (3)$$

and

$$\mathrm{d}Q_f = 4\rho a_f'(1-a_f)U_\infty \pi r^3 \Omega_f \mathrm{d}r \quad (4)$$

where a_f is the axial induction factor of the front rotor, a_f' is the tangential induction factor of the front rotor and Ω_f is the rotation speed of the front rotor.

If the induced velocity (U_{2i}) influence is considered, equation (3) and (4) are modified to

$$\mathrm{d}T_f = 4\rho U_\infty a_f(U_\infty - U_{2i})(1-a_f)\pi r \mathrm{d}r \quad (5)$$

And

$$\mathrm{d}Q_f = 4\rho a_f'(1-a_f)(U_\infty - U_{2i})\pi r^3 \Omega_f \mathrm{d}r \quad (6)$$

The self-induced velocity of the rear turbine is defined as

$$U_{2i} = a_r U_{2,\infty}\gamma \quad (7)$$

where a_r is the axial induction factor of the rear rotor According to [15]

$$\gamma = 1 - \left(\frac{x/r_a}{\sqrt{1+x/r_a}}\right)^{0.3} \quad (8)$$

It is assumed that the rear rotor operates inside stream tube of the front rotor wake, which means

$$U_{2,\infty} = U_{w3} \tag{9}$$

The thrust and torque of the rear are

$$\mathrm{d}T_r = 4\rho U_{w3}^2 a_r(1-a_r)\pi r \mathrm{d}r \tag{10}$$

and

$$\mathrm{d}Q_f = 4\rho a_r'(1-a_r)U_{w3}\pi r^3 \Omega_r \mathrm{d}r \tag{11}$$

where a_r' is the tangential induction factor of the rear rotor and Ω_r is the rotation speed of the rear rotor.

The Prandtl tip loss correction factor [16] is introduced to the forces above to represent the turbine's efficiency loss in BEMT due to the tip-loss effect in the blade root and tip region.

As the turbine enters its turbulent wake state during high axial induction factors at high TSRs, the original BEMT theory will under predict the thrust on the rotor. This can be corrected by using an empirical formulation of the axial induction factor at large a-values, which is obtained from experimental data. Buhl's high induction factor correction is applied to this model, which addressed the issue that high induction corrections fail to incorporate the Prandtl loss factor by fitting a parabolic curve to the highly loaded experimental turbine data [17].

III. Result and Discussion

The parametric study for the counter-rotating tidal turbine is performed by using the Energy System Research Unit (ESRU) in-house BEMT. The parameter of the front rotor is fixed as presented in [18] which is shown in Table I.

TABLE I
THE PARAMETERS OF THE TURBINE

Quantity	Unit
Front rotor radius	0.41m
Rear rotor radius	0.385m
Hub radius	0.1m
Front rotor blade number	3
Rear rotor blade number	4
Blade profile	NRELs814
Front blade pitch	2°
Rear blade pitch	2°
U_∞	0.8m/s
Front rotor section solidity	0.035 to 0.334
Rear rotor section solidity	0.017 to 0.272

In this particular scenario, the distance between the two rotors, denoted as x, is set to be 0.4 times the radius of the rotor (r). This choice of distance ensures that the wake model exhibits a similar trend as presented in reference [13], Fig. 3 showcases an example of the wake velocity deficit for the front rotor at a tip-speed ratio (TSR) of 3. It's important to note that in this schematic, the self-induced velocity of the rear turbine is not taken into account.

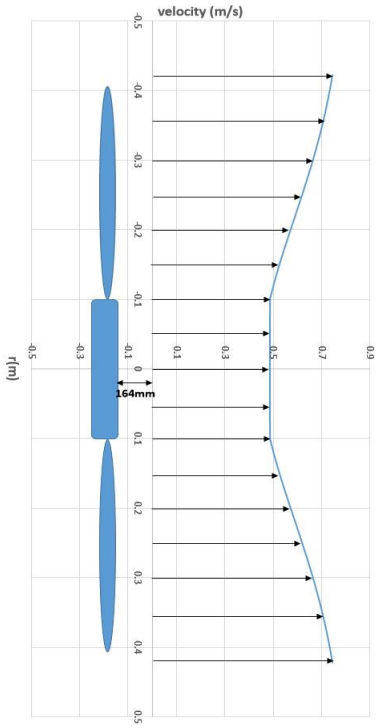

Fig. 3. Wake velocity deficit schematic of the front rotor at Plane 3 ($x = 164mm$).

A. Power Curve

In the design under consideration, the rear rotor is equipped with four blades, each having a radius of 0.385m. The section solidity of the rear rotor spans from 0.017 to 0.272, as indicated by reference [18]. Importantly, the tip-speed ratio (TSR) of the rear rotor is set to be equal to that of the front rotor. The power coefficient (C_P) values achieved by each rotor are depicted in Fig. 4.

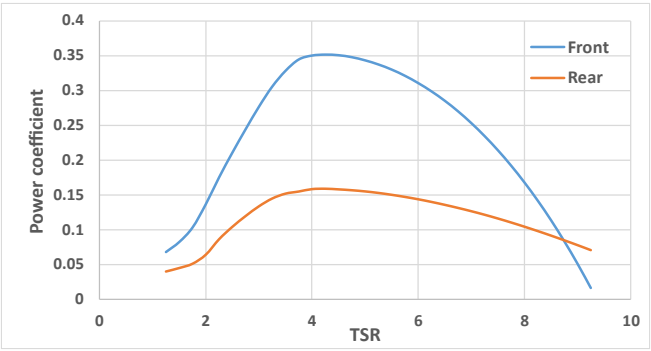

Fig. 4. Power coefficient of each rotor.

The decrease in inflow velocity significantly impacts the power output of the rear rotor, as its blade design is optimized for a constant inflow velocity of 0.8m/s. This is evident from the noticeably lower power output of the

rear rotor compared to the front rotor. Furthermore, the torques exerted on the rear rotor are insufficient to achieve a torque balance across the entire turbine, as depicted in Fig. 5.

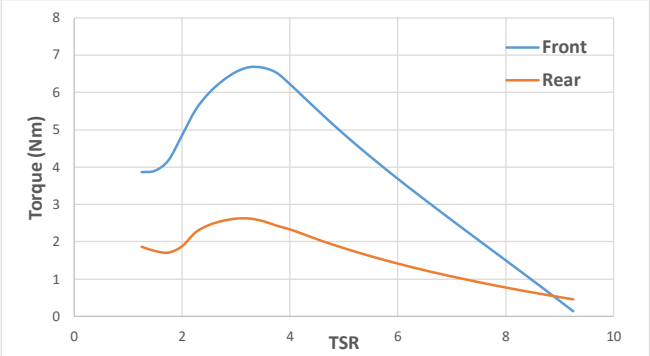

Fig. 5. Torques of each rotor.

B. *Rear rotor modification*

To enhance the torque generation of the rear rotor under decreased inflow conditions, several modifications were implemented in the blade design. Firstly, adjustments were made to the section solidities of the blade, allowing it to effectively operate within the wake region created by the front rotor. Additionally, the twist of the sections was reduced to achieve an optimal angle of attack. Notably, the new section solidities of the rear rotor range from 0.0618 at the tip section to 0.817 at the root section, with a focus on accommodating the low inflow velocity region, Table II shows the differences between two rear blades. As a result, the revised blade design encompasses a wider span compared to the original design, thereby improving its performance in the reduced inflow scenario.

TABLE II
BLADES DISTRIBUTION

	ORIGINAL		MODIFICATION	
SECTION	CHORD	TWIST	CHORD	TWIST
1	0.040136	22.15	0.12833	31.12
2	0.037099	16.34	0.10742	23.8
3	0.033453	11.44	0.09143	18.58
4	0.028752	7.18	0.07913	14.73
5	0.02478	4.04	0.0697	11.79
6	0.021439	2.41	0.06191	9.49
7	0.018983	1.4	0.05576	7.65
8	0.016833	0.99	0.05084	6.14
9	0.014373	0.65	0.04674	4.89
10	0.012299	0.4	0.04305	3.83
11	0.010281	0.25	0.03977	2.92

The power coefficient curve of the new designed turbine is given in Fig, 6, C_p is the overall power coefficient and the tip speed ratio $\lambda = \lambda_1 + \lambda_2$.

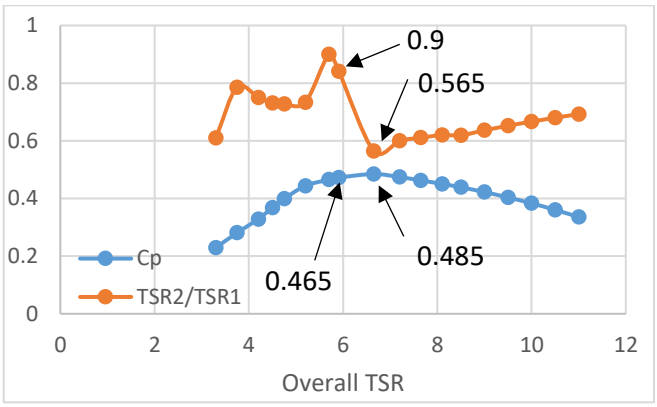

Fig. 6. Overall power coefficient of the rotors and the TSR ratio of the two rotors.

The optimum power coefficient C_p does not correspond to the sum of the highest C_p values achieved by each rotor individually (≈ 0.52), as depicted in Fig. 4. This discrepancy arises from the decrease in rotating speed of the rear rotor, which is necessary to attain an appropriate angle of attack (AoA) capable of generating sufficient torque. Consequently, the AoA of the rear rotor is smaller compared to that of the baseline rotor, which operates at its peak performance. In the modified blade design of the rear rotor, the design tip-speed ratio (TSR) is set at 3, and the torques are balanced at 90% of the designed value (2.7). However, it is important to note that the highest C_p is not obtained at the design TSR ratio. The substantial gap between the design TSR and the TSR at which the highest C_p is achieved indicates the challenge of achieving torque balance between the two rotors within this range.

C. *Pitch and rotating speed*

The turbine's performance was simulated under various blade pitch settings, considering modifications to achieve torque balance. Fig. 7 illustrates the relationship between the power coefficient and the overall TSR. In order to investigate the impact of different blade pitch configurations, four distinct pitch sets were examined, as presented in Table III.

TABLE III
BLADE PITCHES

PITCH SET	FRONT BLADES	REAR BLADES
1	2 DEGREES	2 DEGREES
2	2 DEGREES	0 DEGREES
3	0 DEGREES	0 DEGREES
4	0 DEGREES	2 DEGREES

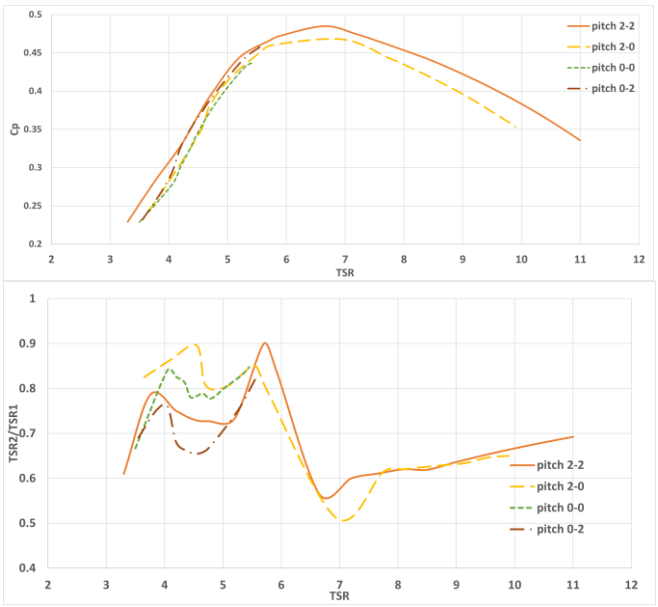

Fig. 7. Overall power coefficient and TSR ratio of the rotors with different blade pitch

Pitch sets 1 and 2 resulted in complete power curves during the simulations, and as anticipated, the optimum design with pitch set 2-2 exhibited the highest power coefficient C_p. However, there remains a discrepancy between the design TSR and the optimal TSR within set 2. On the other hand, simulations were unable to achieve torque balance in pitch sets 3 and 4 as the overall TSR approached the design value. This outcome can be attributed to the fact that the modified blade sections of the rear rotor were designed based on the wake flow of the front rotor, considering a pitch of 2 degrees and accounting for the self-induced velocity effect.

Additionally, it is worth noting that the baseline design TSR for both rotors is $\lambda = 3$. Fig. 8 illustrates the variation in wake deficits of the front rotor, considering the self-induced velocity effect of the rear rotor, across all pitch sets at the baseline design TSR. In pitch sets 1 and 2, the wake deficit velocity profiles are quite similar and notably higher compared to the original wake deficit without considering the self-induced velocity, except in the tip region. However, for pitch sets 3 and 4, there is a decrease in wake velocities. This observation helps explain the inability to find a torque balance point during the simulation when the TSR reaches the baseline design value. Furthermore, it demonstrates that the pitch angle of the rear rotor has a minor influence on its self-induced velocity effect on the wake flow of the front rotor.

Fig. 8. Wake deficit of front rotor at $\lambda_1 = 3$, $\lambda_2 = 3$ of different conditions, the original wake deficit is the condition without self-induced velocity of rear rotor at pitch set 1. 1) the wake deficit with self-induced velocity of rear rotor at pitch set 1. 2) the wake deficit with self-induced velocity at pitch set 2. 3) the wake deficit with self-induced velocity at pitch set 3. 4) the wake deficit with self-induced velocity at pitch set 4.

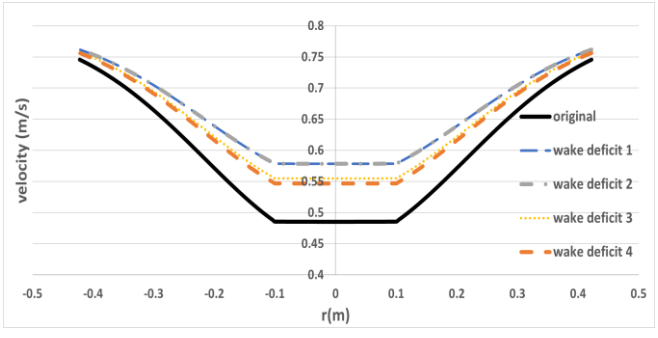

IV. CONCLUSION

The application of a Gaussian-shaped velocity deficit wake model to the Blade Element Momentum Theory (BEMT) facilitated the simulation of the counter-rotating turbine dynamics. This was achieved by determining the inflow velocities for both the front and rear turbines, allowing for a comprehensive analysis within the BEMT framework.

Considering the wake effect generated by the front turbine, it becomes necessary to modify the blade design of the rear rotor to effectively operate under the conditions of reduced inflow velocity. The power coefficient exhibits an increase when the total power is shared between the rotors at the torque balanced point, as opposed to maximizing power extraction solely from the front rotor. Additionally, optimizing the power coefficient involves reducing the rotating speed of the rear rotor to restore the angle of attack and enhance its overall performance. To bridge the gap between the design value and the maximum C_p value. The pitch angle of the front rotor shows a significant effect to the total performance, because the wake velocity will be changed and the rear rotor performance is affected by this velocity.

REFERENCES

[1] S. Lee, E. Son and S. Lee, "Velocity Interference in The Rear Rotor of A Counter-rotating Wind Turbine," *Renewable Energy,* pp. 235-240, 2013.

[2] B. Hwang, S. Lee and S. Lee, "Optimization of A Counter-rotating Wind Turbine Using The Blade Element and Momentum Theory," *Journal of Renewable and Sustainable Energy,* vol. 5, no. 5, p. 052013, 2013.

[3] X. Wei, B. Huang, P. Liu, T. Kanemoto and L. Wang, "Experimental Investigation Into The Effects of Blade Pitch Angle and Axial Distance on The Performance of A Counter-rotating Tidal Turbine," *Ocean engineering,* vol. 110, pp. 78-88, 2015.

[4] B. Huang and T. Kanemoto, "Performance and internal flow of a counter-rotating type tidal stream turbine," *Journal of Thermal Science,* vol. 24, pp. 410-416, 2015.

[5] B. Huang, Y. Nakanishi and T. Kanemoto, "Numerical and experimental analysis of a counter-rotating type horizontal-axis tidal turbine," *Journal of Mechanical Science and Technology,* vol. 30, pp. 499-505, 2016.

[6] K.-M. Dong and S.-N. Jung, "Aerodynamic Performance Prediction of a Counter-rotating Wind Turbine System with Wake Effect," *Journal of the Korean Society for Aeronautical and Space Sciences,* vol. 30, no. 7, pp. 20-28, 2002.

[7] S. N. Jung, T.-S. No and K.-W. Ryu, “Aerodynamic performance prediction of a 30 kW counter-rotating wind turbine system,” *Renewable Energy,* vol. 30, no. 5, pp. 631-644, 2005.

[8] S. Lee, H. Kim, E. Son and S. Lee, "Effects of Design Parameters on Aerodynamic Performance of A Counter-rotating Wind Turbine," *Renewable Energy,* vol. 42, pp. 140-144, 2012.

[9] E. Abohamzeh, M. Jamil and A. C. Benim, “Prediction of Aeroacoustic Performance of Counter-rotating Wind Turbine By Changing The Rotational Speed of Front Rotor,” *SN Applied Sciences,* vol. 2, pp. 1-16, 2020.

[10] M. Bastankhah and F. Porté-Agel, “A New Analytical Model for Wind-turbine Wakes,” *Renewable energy,* vol. 70, pp. 116-123, 2014.

[11] M. Abkar and F. Porté-Agel, “Influence of atmospheric stability on wind-turbine wakes: A large-eddy simulation study,” *Physics of Fluids,* vol. 27, no. 3, 2015.

[12] M. Ge, Y. Wu, Y. Liu and X. I. Yang, “A Two-dimensional Jensen Model with A Gaussian-shaped Velocity Deficit,” *Renewable Energy,* vol. 141, pp. 46-56, 2019.

[13] X. Wei, B. Huang, P. Liu, T. Kanemoto and L. Wang, “Near wake study of counter-rotating horizontal axis tidal turbines based on PIV measurements in a wind tunnel,” *Journal of Marine Science and Technology,* vol. 22, pp. 11-24, 2017.

[14] N. O. Jensen, A note on wind generator interaction, Citeseer, 1983.

[15] J. a. R. O. Yana, “Performance analysis of a coaxial rotor system in hover: Three points of view,” in *Paper presented 28th International Congress of Aeronautical Sciences*, ICAS, 2012.

[16] R. M. J. N. S. C. B. Wen Zhong Shen, “Tip loss corrections for wind turbine computations,” *Wind Energy: An International Journal for Progress and Applications in Wind Power Conversion Technology,* vol. 8, no. 4, pp. 457-475, 2005.

[17] M. L. Buhl Jr, "New empirical relationship between thrust coefficient and induction factor for the turbulent windmill state," National Renewable Energy Lab, Golden, 2005.

[18] J. A. a. C. G. a. G. A. a. J. C. Clarke, “Design and testing of a contra-rotating tidal current turbine,” *Proceedings of the Institution of Mechanical Engineers, Part A: Journal of Power and Energy,* vol. 221, no. 2, pp. 171-179, 2007.